ESR study of mechanism of polyaniline conductivity

A. V. Kulikov, V. R. Bogatyrenko, O. V. Belonogova, L. S. Fokeeva, A. V. Lebedev, T. A. Echmaeva, and I. G. Shunina*

Institute of Problems of Chemical Physics, Russian Academy of Sciences, 14 Institutskii prosp., 142432 Chernogolovka, Moscow Region, Russian Federation. Fax: +7 (096) 515 3588. E-mail: kulav@icp.ac.ru

Powders, solutions, and films of polyanilines synthesized by three methods of aniline oxidative polymerization were studied by ESR, optical spectroscopy, and X-ray diffractometry. Polyanilines under study were shown to differ in the degree of polaron delocalization along solitary polymer chains in a solution, the packing density in powders and films, the mobility of polarons, and the degree of crystallinity. The conductivity of films correlates only with the characteristic time (τ) of O_2 diffusion into amorphous regions of the films. These times were determined from the kinetics of changes in the ESR line intensities after admission of O_2. The higher the film conductivity, the greater the τ value and the sizes of the amorphous regions. The electroconductivity of the films is likely determined by the mobility of polarons in boundary regions between the amorphous regions rather than within the amorphous regions: the larger the sizes of the amorphous regions, the less the number of low-conducting contacts between the amorphous regions and the higher the conductivity.

Key words: polyaniline, morphology, electroconductivity, ESR spectroscopy, molecular oxygen, mobility of polarons.

Conducting polymers, such as polyaniline, polyacetylene, polypyrrole, polyphenylene, and others, are widely used in microelectronic devices, photodiodes, sensors, batteries, technological membranes, *etc*.[1] The main advantage of polyaniline over other conducting polymers is its chemical stability in the presence of oxygen and even in concentrated sulfuric acid. Polyaniline can exist in different forms: a base (**A**), a bipolaron (**B**), and two polarons (**C**).

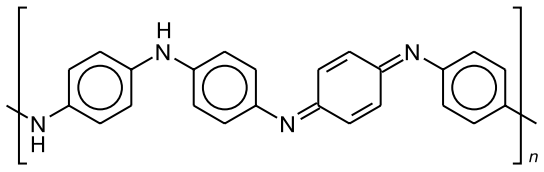

A

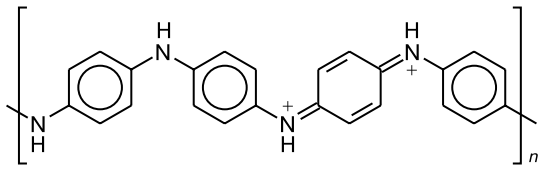

B

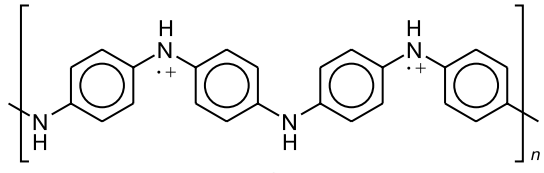

C

The basic form of polyaniline (**A**) contains benzoid and quinoid rings in a ratio of 3 : 1; it is diamagnetic and insulating, and its paramagnetic centers and conductivity appear after its protonation (doping). Protonation results in the appearance of positively charged paramagnetic polarons and diamagnetic bipolarons. Two polarons (**C**) can recombine to form one bipolaron (**B**). Conductivity can be a result of motions of both polarons and bipolarons. Doped polyaniline contains <0.1 paramagnetic sites per two C_6H_4NH units,[2,3] *i.e.*, bipolarons prevail in the polyaniline salt. Nevertheless, the available data[4] indicate that the conductivity occurs mainly through jumps of polarons both along the polymeric chain and between the chains. The X-ray diffraction data showed (see, *e.g.*, Refs. 5—8) that polyaniline contains crystalline and amorphous regions. According to the modern concepts,[9—11] polarons rapidly move within the crystalline regions, and their motion is slow within the amorphous regions, *i.e.*, the conductivity is limited by the motion of polarons in the amorphous regions. In both regions, polarons rapidly jump along polymer chains and slowly between adjacent chains. Therefore, we could expect an increase in the conductivity as the degree of crystallinity increases. However, according to the published data,[7] the conductivity is almost independent of the crystallinity, and for some

Published in Russian in *Izvestiya Akademii Nauk. Seriya Khimicheskaya,* No. 12, pp. 2057—2064, December, 2002.

1066-5285/02/5112-2216 $27.00

polyaniline samples the conductivity even decreases with the crystallinity increase.[8]

The purpose of this work is a search for a correlation between the conductivity of the films and their properties, *viz.*, the delocalization of polarons along the polymeric chain, the density of chain packing, the frequency of jumps of polarons, and the sizes of the amorphous regions.

In this work, powders, solutions, and films of polyaniline synthesized by three methods of aniline polymerization were studied by ESR, optical spectroscopy, and diffractometry. The study of the ESR line shape as a function of the O_2 pressure and the kinetics of O_2 penetration into polyaniline, allows one to reveal the crystalline and amorphous regions of the polymer and to estimate their relative sizes.

Experimental

Three types of polyaniline (PAN-1, PAN-2, and PAN-3), obtained by the oxidative polymerization of aniline under different conditions, were studied. Polyaniline PAN-1 was synthesized for 2 h at ~20 °C in water containing aniline (0.1 mol L^{-1}), $(NH_4)_2S_2O_8$ (0.08 mol L^{-1}), and $HClO_4$ (0.1 mol L^{-1}). The PAN-2 sample was prepared for 5 h at −5 °C in MeCN containing aniline (1 mol L^{-1}) and $HClO_4$ (1 mol L^{-1}) with the gradual addition of $(NH_4)_2S_2O_8$ (1 mol L^{-1}). The PAN-3 sample was synthesized in MeCN at −5 °C with the gradual addition of tetrabutylammonium persulfate as an oxidant according to a previously published method.[12] The polyaniline precipitates were washed several times with MeCN, water, and 0.1 *M* $HClO_4$ (to obtain the acid salt of polyaniline) or 0.1 *M* NaOH (to obtain the polyaniline base) and dried at 40 °C.

The degree of protonation was determined as the ratio y = [Cl]/[N]. The y value was changed by the variation of the time of washing with 0.1 *M* $HClO_4$ or 0.1 *M* NaOH.

Films were prepared from the PAN-1, PAN-2, and PAN-3 powders using *m*-cresol and camphorsulfonic acid (CSA) according to the published method.[13] The basic form of emeraldin was mixed with CSA in the ratio corresponding to the degree of protonation 0.6, then this mixture was dissolved in *m*-cresol, and the solution was dried on a glass support.

The conductivity of the films was determined by the four-point method at a frequency of 1 kHz, and gold electrodes were mechanically pressed to the film. The film thickness (30—50 micron) was determined using a micrometer.

X-ray diffraction patterns were measured on an ADP-1 setup (Russia) at the wavelength of Cu-Kα (λ = 1.5418 Å).

ESR spectra in a 3-cm range were recorded on an SE/X 2544 spectrometer (Radiopan, Poland) under the conditions excluding their distortion. Electronic spectra were obtained on Specord M-40 (Carl Zeiss Jena, Germany) and SF-8 (LOMO, Leningrad) spectrometers.

Before the admission of oxygen, all polyaniline samples were evacuated for 1 h at a pressure of $1 \cdot 10^{-3}$ Torr.

According to the data of mass spectrometric analysis, the oxygen used contained nitrogen (3%), argon (3%), and water vapor (≤0.3%).

Results and Discussion

The conductivity of the films prepared from PAN-1, PAN-2, and PAN-3 using *m*-cresol and CSA is 1, 30, and 370 S cm^{-1}, respectively.

Polyaniline synthesized at low temperatures with the gradual addition of an oxidant should possess a higher molecular weight[7] and contain less defects distorting bond conjugation. The electronic absorption spectra of solutions of polyaniline in concentrated H_2SO_4 (Fig. 1) exhibit peaks at 290, 515, and 1150 nm. According to the previously published data,[14] the absorption maximum at 1150 nm is caused by polarons, and the greater their delocalization, the longer the long-wave tail of this peak. For PAN-1 synthesized at 20 °C, this peak is remarkably sharper than those for PAN-2 and PAN-3. In the spectrum of PAN-1, the peak at 290 nm assigned to the π—π*-transitions of the benzoid rings[14] is less intense. Therefore, we can conclude that PAN-1 contains less amount of the benzoid rings than PAN-2 and PAN-3. The samples also differ in intensities of the peak at 515 nm attributed to charge transfer between the benzoid and quinoid rings.[14]

The characteristic ESR spectra are presented in Fig. 2, and Table 1 contains the linewidths and asymmetry parameters a/b (ratio of the positive deviation of peaks from the basic line to the negative deviation). The width of the ESR line increases in the series powder—film—solution (see Fig. 2, *a*—*c*). Several days after preparation, a solution of polyaniline in concentrated H_2SO_4 also containing NaCl manifests the intense multicomponent spectrum (see Fig. 2, *d*), which is well simulated under the assumption that polyaniline decomposes to the $[C_6H_4 - NH - C_6H_4]^{\bullet +}$ fragments (see Fig. 2, *e*). The hyperfine structure (HFS) from the N nuclei and protons

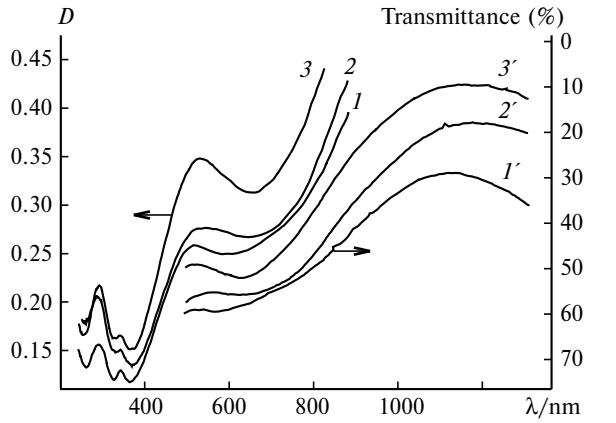

Fig. 1. Electronic absorption spectra of solutions of polyanilines PAN-1 (*1*, *1′*), PAN-2 (*2*, *2′*), and PAN-3 (*3*, *3′*) in concentrated H_2SO_4 in the visible (*1*—*3*) and near-IR regions (*1′*—*3′*). The concentration of polyanilines in all samples was 0.01 mg mL^{-1}.

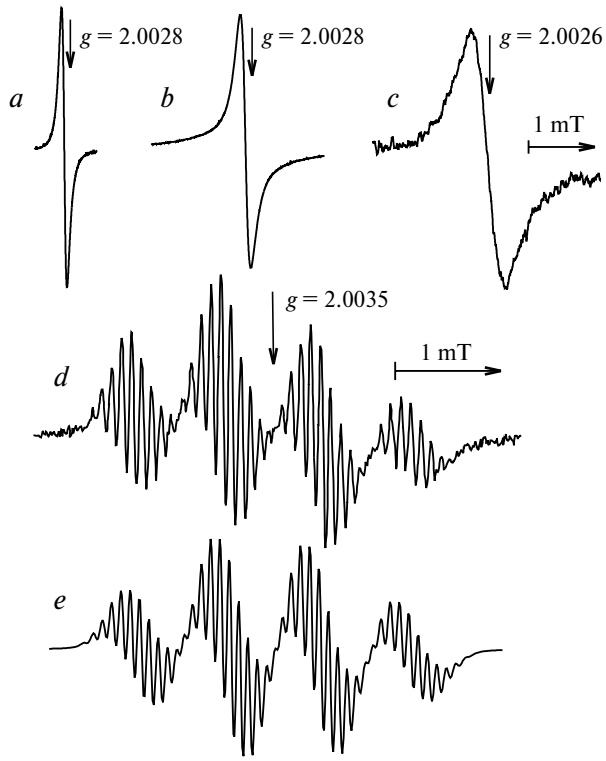

Fig. 2. ESR spectra of PAN-2 at 20 °C: *a*, powder, $y = 0.13$, *in vacuo*; *b*, film, $y = 0.6$; *c*, solution (4 mg mL^{-1}) in concentrated H_2SO_4; *d*, solution in 80% H_2SO_4 with an additive of NaCl, two weeks after dissolution; *e*, simulated spectrum with the HFS constants a_H (1 H) = 0.79 mT, a_H (4 H) = 0.16 mT, a_H (4 H) = 0.086 mT, a_N (1 N) = 0.79 mT, the linewidth in the center is 0.05 mT, the width gradient is 0.04 mT $(mT)^{-1}$.

is not found in the ESR spectra of polyaniline powders, films, and solutions because the HFS constants are low due to the delocalization of polarons. In a solution delocalization occurs along the solitary polymeric chain, and in powders and films delocalization also involves adjacent chains. This delocalization can be both static and dynamic, *i.e.*, caused by fast jumps of polarons. The narrowing of the ESR lines of polyaniline is likely due to the static delocalization of polarons mainly because the linewidth of polyaniline in an inert atmosphere slightly changes at temperatures <100 K when polarons are localized ("pinged").[15—17]

The spectrum of a solution of PAN-1 demonstrates the greatest linewidth (1 mT) due to a lower delocalization of polarons, which agrees with the electronic spectra. At the same time, the ESR line of the PAN-1 powder at $y = 0.32$ in a vacuum has the smallest width, which can be explained by a denser packing of the polymeric chains having smaller molecular weight. In air, the ESR lines broaden (see Table 1) due to the addition of paramagnetic O_2 molecules to the polymeric chains (see Refs. 16—18 and references cited therein). According to the published data,[18] the broadening in air is due to the competition

Table 1. Width and parameters *a*/*b* of ESR lines for different polyaniline samples at 20 °C in a vacuum (I) and air (II)

Sample	Phase	*y* (σ/S cm^{-1})	Width/mT		*a*/*b*	
			I	II	I	II
PAN-1	Powder	0.52	0.082	0.23	1.11	1.11
	Powder	0.32	0.021	0.11	1.09	1.05
	Film	0.6 (1)	0.50	0.55	1.08	1.09
	Solution in H_2SO_4	—	—	1.00	—	1.06
PAN-2	Powder	0.53	0.074	0.105	1.04	1.04
	Powder	0.32	0.092	0.11	1.05	1.07
	Powder	0.13	0.093	0.12	1.05	1.06
	Film	0.6 (30)	0.15	0.17	1.15	1.18
	Solution in H_2SO_4	—	—	0.52	—	1.11
PAN-3	Powder	0.5	0.27	2.28	1.07	1.10
	Film	0.6 (370)	1.0	1.10	1.40	1.70
	Solution in H_2SO_4	—	—	0.52	—	~1.0

between the O_2 and H_2O molecules for bonding sites. If the sample was pre-evacuated, the effect of oxygen significantly increased.

The ESR lines are asymmetric, and parameter *a*/*b* is > 1 (see Table 1). The maximum asymmetry is observed for the films and can be accounted to their high conductivity. The line shape depends on the conductivity and also on the size of the sample.[19] For the films under study with close sizes (~5×10×0.05 mm^3), the conductivity correlates with the *a*/*b* parameter (see Table 1). Note that the *a*/*b* value for the PAN-3 film is higher in air than in vacuum. This is due to an increase in the conductivity of polyaniline under the effect of water vapors.[3,6,20] The powders and solutions are also characterized by a low asymmetry of the ESR line. In this case, the asymmetry cannot be explained by conductivity because the sizes of the samples and their conductivities are small. For PAN-2, this asymmetry arises in part from the superposition of the ESR lines with close *g* factors and is more pronounced when the spectra are recorded in the 2-mm range (Fig. 3, *a*). Similar ESR spectra of polyaniline were ear-

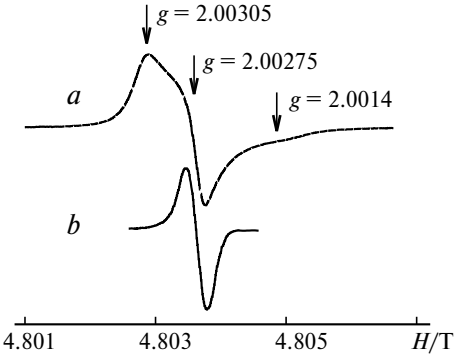

Fig. 3. ESR spectra of polyaniline powders in the 2-mm range at ~20 °C: PAN-2 with $y = 0.52$ (*a*) and PAN-1 with $y = 0.32$ (*b*).

lier[21] observed in this range and explained by the anisotropy of g factor, which decreased with an increase in the degree of doping due to a higher delocalization of the polarons. The ESR spectrum of PAN-1 in the 2-mm range (Fig. 3, *b*) is a solitary line, probably, also due to a denser packing of the chains. In the 3-cm range, the asymmetry is low and the ESR lines have nearly the Lorentz shape, especially when the lines are broadened by O_2.

Thus, the conductivity of the films does not correlate with either the degree of delocalization of polarons along the polymeric chain (estimated from the optical spectra and the ESR line width of a solution of polyaniline in H_2SO_4) or the density of chain packing (estimated from the ESR linewidths in a vacuum).

The diffraction patterns of the powders and films (Fig. 4) show that the films are almost amorphous and the powders are characterized by a low degree of crystallinity. The degree of doping of the powders has almost no effect on their diffraction patterns. The degree of crystallinity of the powders was estimated from the ratio of the surface area of two peaks at $2\theta = 25$ and 27° to the surface area of the whole diffraction pattern after the basic line was subtracted. The peaks were separated by a straight line tangent to the diffraction pattern at 22 and 29°, and the basic straight line matched the zero line of the diffraction pattern at 10 and 60°. The degrees of crystallinity of two powders are presented in Table 2.

Analysis of the relation between the ESR linewidth for the polyaniline powders and the O_2 pressure (Fig. 5) also

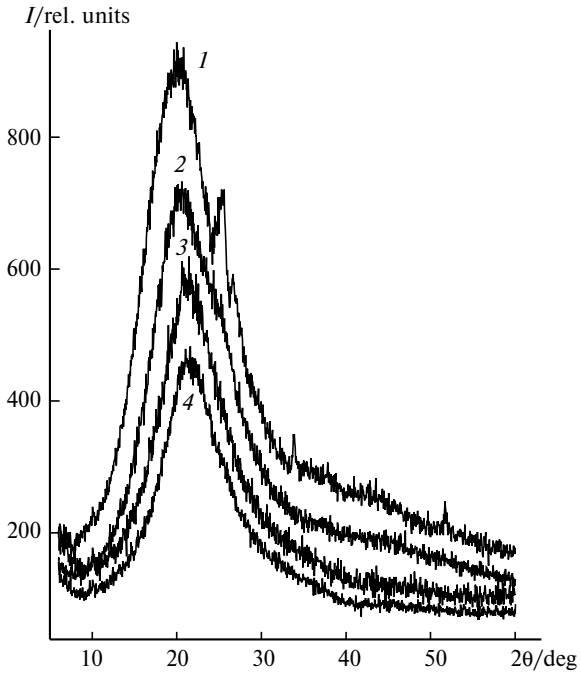

Fig. 4. Diffraction patterns of polyaniline powders and films: powder of PAN-2, $y = 0.13$ (*1*); powder of PAN-1, $y = 0.32$ (*2*); film of PAN-2, $y = 0.6$ (*3*); and film of PAN-3, $y = 0.6$ (*4*).

Table 2. Degrees of crystallinity of polyaniline powders PAN-1 and PAN-2 found from the diffraction pattern (I), isotherm (II), and the ESR line shape (III)

Sample	y	Degree of crystallinity (%)		
		I	II	III
PAN-1	0.32	1.0±0.8	0.6±0.2	1.5±0.6
PAN-2	0.13	3.2±1	2±1	3.5±0.5

Table 3. Parameters of Langmuir isotherms of polyaniline powders and films

Sample	Phase	y (σ/S cm^{-1})	T/K	K/atm	A/mT
PAN-1	Powder	0.32	0	0.01	0.02
				6.3	2.9
PAN-2	Powder	0.13	0	0.01	0.02
				2.9	1.0
PAN-1	Film	0.6 (1)	293	1.0	0.97
PAN-2	Film	0.6 (30)	293	0.39	0.18
PAN-3	Film	0.6 (370)	293	Linear broadening 0.8 mT atm^{-1}	

makes it possible to reveal the amorphous and crystalline regions and estimate the degree of crystallinity. These plots were described by the sum of two Langmuir isotherms

$$\Delta H = \Delta H_0 + \frac{A_1 P}{K_1 + P} + \frac{A_2 P}{K_2 + P}, \qquad (1)$$

where P is the O_2 pressure, and A_i and K_i are constants. The A_i and K_i values for the powders and films are presented in Table 3. The accuracy of these values is ~30%. The constants were determined by fitting with the use of

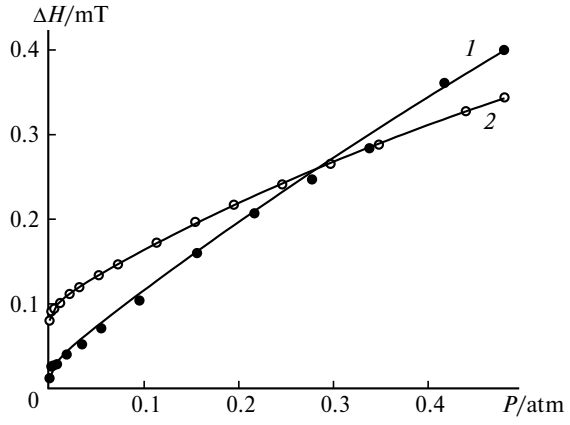

Fig. 5. Plots of the broadening of the ESR spectra (ΔH) of the polyaniline powders PAN-1 with $y = 0.32$ (*1*) and PAN-2 with $y = 0.13$ (*2*) *vs.* dioxygen pressure (P) at 0 °C. The lines correspond to Eq. (1) with the parameters presented in Table 3.

the ORIGIN program. For the films, the plot of the ESR linewidth *vs.* O_2 pressure was described by one isotherm. For the PAN-3 film, the A and K values were not found because the plots of the width *vs.* O_2 pressure was linear. The degrees of crystallinity of two powders determined as the $A_1/(A_1 + A_2)$ ratio are presented in Table 2.

Strictly speaking, representation of the plot of the broadening *vs.* O_2 pressure by formula (1) is valid if the delocalization and motions of polarons average the effect of the oxygen molecules. In this case, the linewidth is proportional to the mean concentration of oxygen in polyaniline, the terms in formula (1) correspond to two sites of oxygen bonding, and the ESR line is Lorentzian in shape at any O_2 pressure. In our case, the ESR lines for some samples are the sum of two lines with different widths, which refer to the crystalline and amorphous phases. Therefore, to determine the degree of crystallinity, one has to analyze the line shape on the basis of strong difference between the K_1 and K_2 constants in Eq. (1). Gradually admitting oxygen to an evacuated sample, one can find such a pressure at which the narrow signal completely disappeared and the remaining broad signal was not strongly broadened. Then the difference of the signals *in vacuo* and under thus determined oxygen pressure gives a narrow ESR line from the crystalline phase, and the degree of crystallinity can be calculated from the ratio of second integrals of the narrow signal and the line *in vacuo*. Example of such a subtraction of the spectra for the PAN-1 powder is shown in Fig. 6, and the degrees of crystallinity determined from the ratio of the second integrals are presented in Table 2. It is seen that the degrees of crystallinity of the powders obtained by three methods satisfactorily agree with each other.

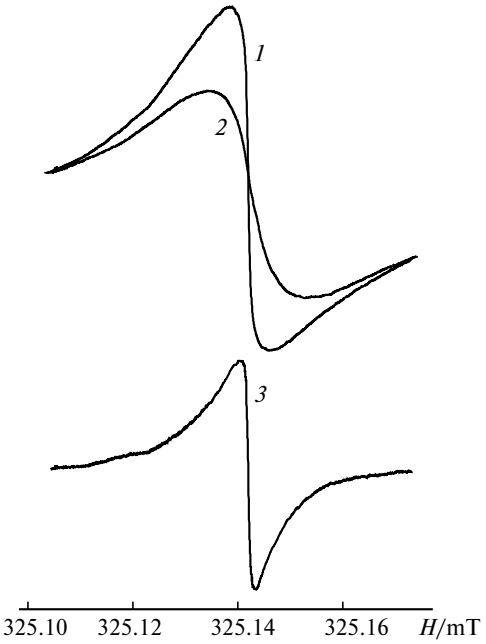

Fig. 6. ESR spectra of the PAN-1 powder with $y = 0.32$ at 20 °C: *1*, *in vacuo*; *2*, at the O_2 pressure of 0.004 atm; and *3*, difference in spectra *1* and *2*.

The degrees of crystallinity of the films are low and do not exceed 0.5%. At the same time, the conductivity of the PAN-3 film is higher than those for other films also synthesized[8] using CSA and *m*-cresol but characterized by the 20—40% degree of crystallinity. No correlation between the degree of crystallinity and conductivity was found in several works.[7,8] Therefore, crystallinity is not the main conductivity-determining parameter.

The temperature plots of the ESR linewidths for the films in the presence of oxygen are presented in Fig. 7. The main peculiarities of the O_2 influence on the ESR linewidth can be explained by the model,[22] according to which the paramagnetic O_2 molecule adds to the polymer, and the exchange interaction in the moment of collisions between the spins of the immobile dioxygen molecule and a mobile polaron results in broadening. Thus, the mobility of polarons along the polymeric chain can be estimated studying the oxygen broadening. The first estimates of frequencies of polaron jumps in polyaniline were obtained[22] from the ESR linewidth at a fixed temperature. We have previously[16] found a maximum in the temperature plot of the oxygen broadening for the PAN-2 powder. This maximum was accounted for the transition from fast exchange to slow exchange due to a decrease in

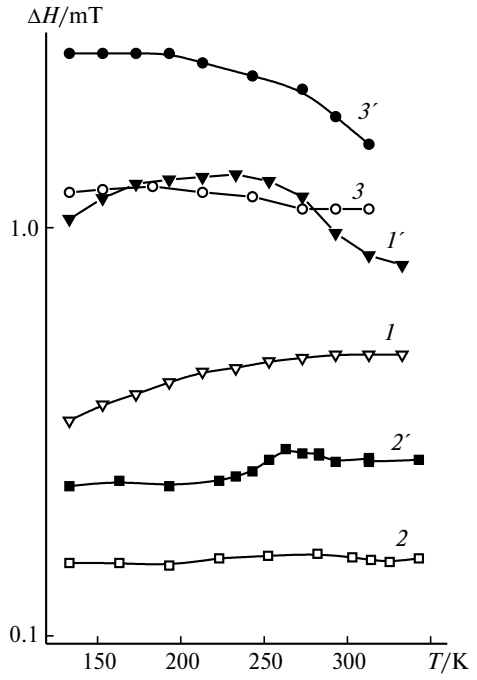

Fig. 7. Plots of the linewidth (ΔH) of the polyaniline films of PAN-1 (*1*, *1′*), PAN-2 (*2*, *2′*), and PAN-3 (*3*, *3′*) *vs.* temperature *in vacuo* (*1—3*) and in the presence of oxygen (*1′—3′*) at $P = 0.50$ (*1′*), 0.52 (*2′*), and 0.88 atm (*3′*). The ordinate axis is logarithmic.

the mobility of polarons with the temperature decrease. The presence of this maximum enhances the reliability of estimation of the polaron mobility. The higher the mobility of polarons, the lower the temperatures at which this maximum is observed. The maximum in curve *2* corresponds to the higher temperature than that in curve *1*, which can be attributed to a lower mobility of polarons in the PAN-2 film compared to that in the PAN-1 film. For PAN-3, the maximum is probably observed at lower temperatures and, hence, the mobility of polarons in PAN-3 is higher than that in PAN-1. Thus, the mobility of polarons increases in the series PAN-2 < PAN-1 < PAN-3 and does not correlate to the conductivity of these films, which increases in the series PAN-1 < PAN-2 < PAN-3.

This analysis is valid if the amount of oxygen sorbed by polyaniline remains unchanged with temperature variation. However, in the case of the polyaniline powders, one has to take into account[17] a change in the amount of sorbed oxygen with temperature variation. For the polyaniline films, unlike the powders, the amount of sorbed oxygen remains virtually unchanged (see below).

Our experiments showed that the conductivity of the films correlates with the time of oxygen penetration into the film. The study of the kinetics of changing the amount of sorbed oxygen allows the estimation of the relative sizes of the polyaniline particles. Typical kinetic curves for the powders are presented in Fig. 8. The kinetics was measured by the temperature jump down by 20—30 K. At temperatures >220 K the amplitude of the line decreases very rapidly after the jump (not shown in the figure) due to fast addition of oxygen until the equilibrium (at a given temperature) concentration is achieved, and then it increases rather slowly due to the displacement of oxygen by water. The amplitude only rapidly decreases in the absence of water. At lower temperatures the pressure of saturated water vapor is low, and we observed only the kinetics of oxygen addition, which is limited by the diffusion of O_2 into the polyaniline particles. When the temperature jumps up (instead of jump down), the increase in the amplitude changes to a decrease, whereas the decrease is replaced by an increase. The kinetic curves are well described by the formula $A = A_0 + \Delta A\exp(-t/\tau)$ (see Fig. 8). As known,[23] for the diffusion of particles into spherical or cylindrical regions, the kinetics of changing the mean concentration (C) of particles in these regions obeys the law $\Delta C/\Delta C_0 \sim \exp(-t/\tau)$, where $\tau \sim R^2/D$, R is the radius of the region, and D is the diffusion coefficient. This relation holds at sufficiently long times t or short radii R. In our case, the broadening of the ESR line under the oxygen effect is proportional to the mean concentration of oxygen in polyaniline. At the O_2 pressures >0.02—0.04 atm, the line shape is close to the Lorentz one, the product of the amplitude by the squared linewidth is constant, and the exponential kinetics of changing the ΔH values results in the exponential kinetics of changing the amplitude. In this work, we measured the kinetics of changing the amplitude because the amplitude can be measured more accurately than the width.

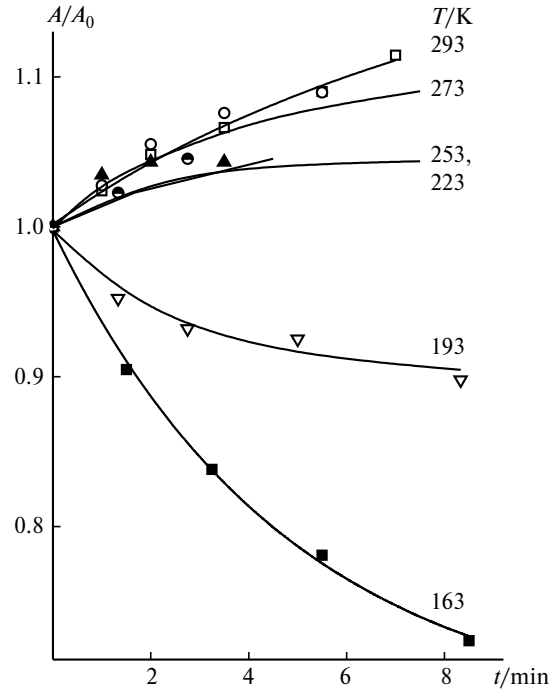

Fig. 8. Plots of the amplitude of the ESR line (A) of the PAN-2 powder with $y = 0.13$ *vs.* time after the temperature jump. The sample was evacuated and filled at 20 °C with a mixture of O_2 (0.055 atm) and water vapor (0.011 atm). The lines are exponents drawn through experimental points.

The Arrhenius plots of the characteristic times τ for the powders are shown in Fig. 9. The dotted lines represent the data obtained in the presence of water. For PAN-2 the τ values in both the absence and presence of water are higher by 3—4 times than those for PAN-1. In our opinion, this can be explained by the fact that the PAN-2 particles are larger. The τ values depend slightly on the degree of doping, *i.e.*, the particle size is mainly determined by the conditions of synthesis, and a change in the degree of doping of the already synthesized polyaniline slightly changes the particle sizes.

In the presence of water vapor at high temperatures (see Fig. 8), changes in the amplitude are determined by diffusion of water molecules. The characteristic times for diffusion of the water, unlike other times, increase with a decrease in the temperature (see Fig. 9, lines *6* and *8*). In the case of chemical reactions, negative activation energies for the reaction rate constant indicate that the reaction is not elementary and consists of at least two steps.[24] For such processes in polymeric materials as the penetration of gases through membranes, the step of gas dissolution and the diffusion step should be included into consideration.[25] The solubility increases with the temperature decrease, and if the rate of gas dissolution in the

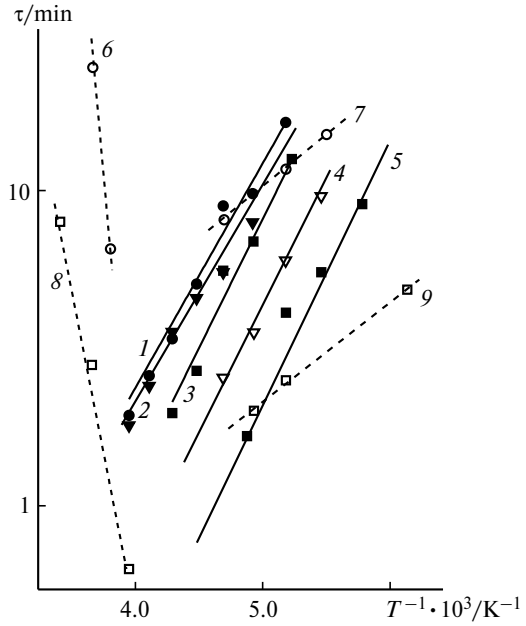

Fig. 9. Arrhenius plots of the characteristic time (τ) of changing the amplitude of the ESR lines of the polyaniline powders in the presence of O_2 (0.5 atm) after the temperature jump: PAN-2 with $y = 0.13$ (*1*), 0.52 (*2*), and 0.32 (*3*); PAN-1 with $y = 0.52$ (*4*) and 0.32 (*5*); PAN-2 with $y = 0.13$ (*6* and *7*) in the presence of 0.012 atm of water vapor; PAN-1 with $y = 0.32$ (*8* and *9*) in the presence of 0.012 atm of water vapor. Plots *6*, *8* and *7*, *9* were obtained in different temperature intervals and reflect diffusion of water vapor (*6*, *8*) and oxygen (*7*, *9*) (see text). The ordinate axis is logarithmic.

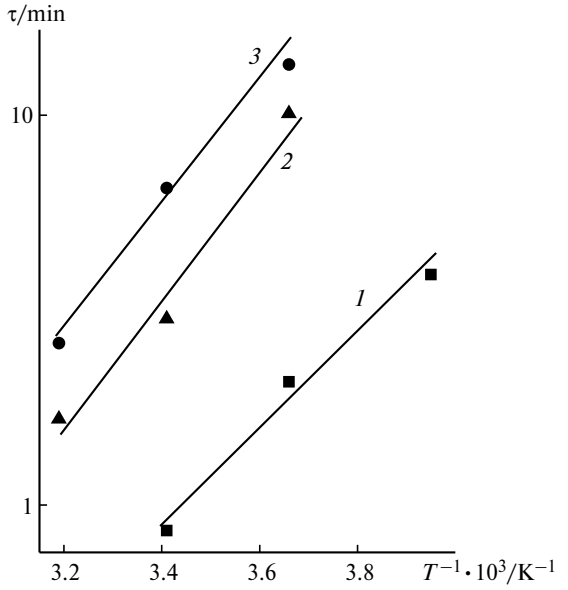

Fig. 10. Arrhenius plots of the characteristic time (τ) of changing the amplitude of the ESR line of polyaniline films after the addition of 0.5 atm of oxygen: PAN-1, film conductivity 1 S cm^{-1} (*1*), PAN-2, 30 S cm^{-1} (*2*), and PAN-3, 370 S cm^{-1} (*3*).

matrix (between particles) is comparable with the rate of diffusion into particles, the rate of increasing the mean concentration of gases in the particles can increase with the temperature decrease. Solubility should be taken into account for oxygen bound to polyaniline: the K constants in Eq. (1) are proportional to the product of the solubility by the true gas—bound gas equilibrium constant.

In the presence of water vapor, the activation energy of oxygen diffusion decreases (see Fig. 9, lines *1*—*5*, *7*, and *9*). This can be explained by the fact that in polymers diffusion occurs by jumps between bonding sites, and the bonding energy determines the activation energy. Water occupies some potential bonding sites, and sites with a lower energy of oxygen bonding remain free.

The kinetics of oxygen addition to the polyaniline powders can be studied after the jumps of both the temperature and pressure. In the case of the films, the kinetics of changing the amplitude was measured after the pressure jump because, unlike the powders, the interval of the amplitude change ΔA was <5% at the temperature jump by 20 K. The characteristic times for the films correlate well with their conductivity: the times are longer for the films with a higher conductivity (Fig. 10). The time values can differ due to differences in both the sizes of polyaniline particles and the diffusion coefficients. Differences in the diffusion coefficients are less probable because the activation energies should also change in this case. However, the slopes of the straight lines in Fig. 10 are close. Thus, the high-conducting films have large sizes of particles. This can be explained by the supposition that the conductivity is limited by the diffusion of polarons in the boundary regions between the amorphous regions rather than in the amorphous regions as it was earlier believed[9—11]: the larger the sizes of the amorphous regions, the less the

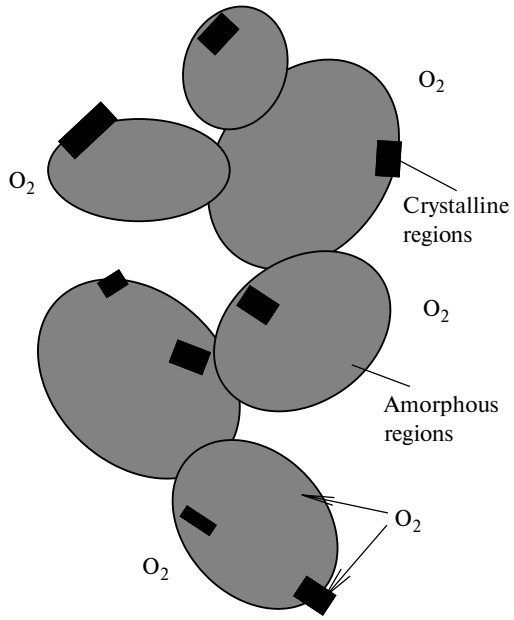

Fig. 11. Supramolecular structure of polyaniline.

number of low-conducting contacts between them and the higher the conductivity (Fig. 11).

The globular polyaniline structure doped with CSA with the globule size from 10 to 1000 nm was observed[26] by scanning electron microscopy. It was found by standard porosimetry[27] that the pore radius in polyaniline is 1—100 nm and the mean radius of fibrils is 2—10 nm. Thus, the sizes of the polyaniline particles have a broad distribution, and the τ values determined by the ESR method reflect the mean particle sizes.

The authors thank M. G. Kaplunov for recording electronic spectra in the near-IR region, V. I. Krinichnyi and M. R. Zhdanov for recording ESR spectra in the 2-mm range, and the Center of Collective Using at the Institute of Chemical Physics of the RAS (supported by the Russian Foundation for Basic Research, Project No. 00-03-40141) for obtaining diffraction patterns.

This work was financially supported by the Russian Foundation for Basic Research (Project No. 98-03-33140a).

References

1. *Intern. Conf. on Science and Technology of Synthetic Metals*, (a) *July 14—21, 2000, Gastein, Austria*, *Book of Abstracts*, Gastein, 2000, (b) *July 28—August 2, 1996, Snowbird, Utah*, in *Synthetic Metals*, 1997, **84**, No. 1—3, (c) *July 24—29, 1994, Seoul, Korea*, in *Synthetic Metals*, 1995, **68—70**.
2. A. J. Epstein, J. M. Ginder, F. Zuo, H. S. Woo, D. B. Tanner, A. F. Richter, M. Angelopolos, W. S. Huang, and A. G. Mac Diarmid, *Synth. Met.*, 1987, **21**, 63.
3. A. V. Kulikov, Ya. L. Kogan, and L. S Fokeeva, *Synth. Met.*, 1995, **69**, 223.
4. (a) O. Chauvet, S. Paschen, L. Forro, L. Zuppiroli, P. Bujard, K. Kai, and W. Werner, *Synth. Met.*, 1994, **63**, 115; (b) Y. Furukava, *J. Phys. Chem.*, 1996, **100**, 15644; (c) K. Mizoguchi and S. Kuroda, in *Handbook of Organic Conductive Molecules and Polymers*, Ed. H. S. Nalva, J. Wiley and Sons, Chichester—New York, 1997, **3**, 231.
5. M. E. Josefowich, R. Laversanne, H. H. S. Javadi, A. J. Epstein, J. P. Pouget, X. Tang, and A. G. MacDiarmid, *Phys. Rev.*, *B*, 1989, **39**, 12958.
6. B. Z. Lubentsov, O. N. Timofeeva, S. V. Saratovskikh, V. I. Krinichnyi, A. E. Pelekh, V. I. Dmitrienko, and M. L. Khidechel, *Synth. Met.*, 1992, **47**, 187.
7. J. Stejskal, A. Riede, D. Hlavata, J. Prokes, M. Helmsted, and P. Holler, *Synth. Met.*, 1998, **96**, 55.
8. D. Djurado, Y. F. Niccolau, I. Dalsegg, and E. J. Samuelsen, *Synth. Met.*, 1997, **84**, 121.
9. Z. H. Wang, H. H. S. Javadi, A. Ray, A. G. MacDiarmid, and A. J. Epstein, *Phys. Rev.*, *B*, 1990, **42**, 5411.
10. Z. H. Wang, C. Li, E. M. Scherr, A. G. MacDiarmid, and A. J. Epstein, *Phys. Rev.*, *B*, 1992, **45**, 4190.
11. B. Beau, J. P. Travers, and E. Banka, *Synth. Met.*, 1999, **101**, 7772.
12. I. Kogan, L. Fokeeva, I. Shunina, I. Estrin, L. Kasumova, M. Kaplunov, G. Davidova, and E. Knerelman, *Synth. Metals*, 1999, **100**, 3.
13. E. R. Holand, S. J. Pomfret, P. A. Adams, and A. P. Monkman, *J. Phys. Condens. Matter*, 1996, **8**, 2991.
14. S. Folch, A. Gruger, A. Regis, and Ph. Colomban, *Synth. Met.*, 1996, **81**, 221.
15. Z. H. Wang, A. R. MacDiarmid, A. G. MacDiarmid, and A. P. Epstein, *Phys. Rev.*, *B.*, 1991, **43**, 4373.
16. A. V. Kulikov, V. R. Bogatyrenko, O. V. Belonogova, and L. S. Fokeeva, *Izv. Akad. Nauk*, *Ser. Khim.*, 1999, 2293 [*Russ. Chem. Bull.*, 1999, **48**, 2267 (Engl. Transl.)].
17. A. V. Kulikov, V. R. Bogatyrenko, O. V. Belonogova, and L. S. Fokeeva, *Izv. Akad. Nauk*, *Ser. Khim.*, 2000, 1762 [*Russ. Chem. Bull.*, *Int. Ed.*, 2000, **49**, 1742].
18. P. K. Kahol, A. J. Dyakonov, and B. J. McCormick, *Synth. Met.*, 1997, **84**, 691; **89**, 17.
19. F. D. Dyson, *Phys. Rev.*, 1955, **98**, 349.
20. A. Alix, V. Lemoine, M. Nechtschein, J. P. Traders, and C. Meaner, *Synth. Met.*, 1989, **29**, 457.
21. V. I. Krinichnyi, S. D. Chemerisov, and Ya. S. Lebedev, *Phys. Rev.*, *B*, 1997, **55**, 1623.
22. E. Houze and M. Nechtschein, *Phys. Rev.*, *B*, 1996, **53**, 14309.
23. W. Jost, *Diffusion in Solids*, *Liquids and Gases*, Academic Press, New York, 1952.
24. E. T. Denisov, *Kinetika gomogennykh khimicheskikh reaktsii* [*Kinetics of Homogeneous Chemical Reactions*], Vysshaya Shkola, Moscow, 1978, 368 pp. (in Russian).
25. (a) W. J. Koros and M. Moaddeb, *Gas Barrier Polymers*, in *The Polymeric Materials Encyclopedia*, Ed. J. C. Salamone, CRC Press, Boca Raton, 1996; (b) L. M. Robeson, *Gas Separation Membranes*, Ed. J. C. Salamone, CRC Press, Boca Raton, 1996.
26. M.-C. Bernard, A. Hugot-Le Coff, Vu Thi Bich, and Wen Zeng, *Synth. Met.*, 1996, **81**, 215.
27. Yu. M. Volfkovich, A. G. Sergeev, T. K. Zolotova, S. D. Afanasiev, O. N. Efimov, and E. P. Krinichnaya, *Electrochim. Acta*, 1999, **44**, 1543.

Received August 9, 2001;
in revised form April 11, 2002